PHYSICAL REVIEW B **78**, 100102(R) (2008)

Dynamical stability of the cubic metallic phase of AlH_3 at ambient pressure: Density functional calculations

D. Y. Kim,[1,*] R. H. Scheicher,[1] and R. Ahuja[1,2,†]

[1]*Condensed Matter Theory Group, Department of Physics and Materials Science, Box 530, Uppsala University, SE-751 21 Uppsala, Sweden*

[2]*Applied Materials Physics, Department of Materials and Engineering, Royal Institute of Technology (KTH), SE-100 44 Stockholm, Sweden*

(Received 22 August 2008; published 26 September 2008)

We have characterized the high-pressure cubic phase of AlH_3 from *ab initio* using density functional theory to determine mechanical as well as electronic properties and lattice dynamics (phonon-dispersion relations) from the response function method. Our zero-temperature phonon calculations show the softening of a particular mode with decreasing pressure, indicating the onset of a dynamic instability that continues to persist at ambient conditions. This instability can, however, be removed when finite electronic temperature effects are considered in the calculations. We furthermore identify a particular momentum transfer in the phonon-dispersion relation, matching a corresponding momentum transfer in the electronic band structure.

DOI: 10.1103/PhysRevB.78.100102 PACS number(s): 62.50.−p, 63.20.kd, 62.20.D−

Aluminum hydride currently receives increased interest from the scientific community for two reasons. On the one hand, AlH_3 is discussed as a promising hydrogen storage material due to its large gravimetric density of 10 wt %. On the other hand, AlH_3 also belongs to the class of so-called "hydrogen-rich materials," which are expected to be of relevance when studying phenomena related to metallic hydrogen. Recently, a high-pressure metallic phase in AlH_3 with structure of space group $Pm\bar{3}n$ has been predicted theoretically[1] and subsequently also observed experimentally.[2] Besides the obvious importance of this discovery from a fundamental physics point of view, this structure may also be highly relevant for the hydrogen storage aspects of AlH_3 (Refs. 3–9) since the phase was shown[1] to be stable against dehydration. Furthermore, its insulator-metal transition entails a delocalization of electrons, leading to a weakening of Al-H bonds, which in turn results in an effective reduction in the hydrogen removal energy by 75% compared to the insulating phase of AlH_3, as we recently demonstrated from density functional theory and GW calculations.[10]

Here, we focus on the mechanical and dynamical stabilities of this phase. To this end, we have studied phonon-dispersion relations and mechanical properties as a function of pressure. Our zero-temperature calculations demonstrate that cubic AlH_3 is unstable below a certain threshold pressure, preceded by the onset of phonon softening. However, once finite-temperature effects are considered, the system can become dynamically stable even for low-pressure values. Thus, based on our theoretical results, it appears feasible to prepare the cubic phase of AlH_3 at ambient conditions by quenching the high-pressure phase, as it has already been successfully demonstrated in the past by our *ab initio* lattice dynamics calculations[11] in conjunction with diamond-anvil cell (DAC) experiments for the hardest known oxide (cotunnite structured TiO_2).[12]

The computational studies presented here are based on the generalized gradient approximation (GGA) (Ref. 13) of density functional theory (DFT).[14,15] We employed the projector-augmented wave (PAW) approach,[16] as implemented in the well-known VASP code,[17,18] to calculate the pressure as a function of volume and to determine the strain for a range of pressure values. Convergence was achieved with a cut-off energy of 600 eV and a k-point mesh of $21\times21\times21$ generated with the Monkhorst-Pack method.[19] No relaxation of ionic positions was required for the cubic phase of AlH_3 due to the symmetry-based canceling of all internal forces.

To calculate phonon-dispersion relations, density functional perturbation theory was used, in which the Fermi-Dirac (FD) broadening scheme is employed for electronic excitations.[20,21] Calculations in ABINIT (Ref. 22) are based on the local-density approximation (LDA) (Ref. 23) with the norm-conserving pseudopotential technique[24] and plane waves up to a cut-off energy of 120 Ha. To calculate the total phonon-dispersion relation and density of states, a $16\times16\times16$ Monkhorst-Pack[19] k-point mesh was found to yield converged results. Phonon-dispersion curves were calculated along the $\Gamma-X-R-\Gamma-M$ high-symmetry points.

In Fig. 1, we plot the pressure as a function of volume. The third-order Birch-Murnaghan (BM) equation of state (EOS) (Refs. 25 and 26) was used to fit the data, and from this the bulk modulus for the cubic phase of AlH_3 was determined as 52 GPa. In addition, we have also calculated the shear modulus for different pressures by way of tetragonal distortion of the lattice such that the unit-cell volume is kept constant. From a quadratic fit to the energy-distortion relation, we were then able to evaluate the tetragonal and trigonal shear elastic constants $C'=(C_{11}-C_{12})/2$ and C_{44}, which in turn allows us to characterize the stability for different pressures. The results from these calculations are summarized in Fig. 2. As it can be seen, both C' and C_{44} rise proportional to the applied pressure, and remain positive throughout the investigated pressure range. This leads us to the conclusion that the cubic phase of AlH_3 is *mechanically* stable regardless of the applied pressure. However, as we will show in the following, an analysis of the lattice dynamics reveals that the system is found to be actually *dynamically* stable only in the pressure range of 72–106 GPa.

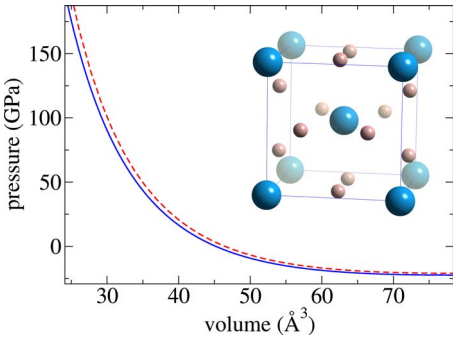

FIG. 1. (Color online) Relation between pressure and volume for cubic AlH_3 as obtained from a third-order Birch-Murnaghan equation of state fit. The solid line represents the fit to the data calculated using ABINIT while the dashed line corresponds to the fit to data obtained using VASP. The inset shows the unit cell of cubic AlH_3 in space group 223 ($Pm\bar{3}n$) (Al at 2*a* sites; H at 6*c* sites) with the larger blue-colored spheres representing Al and the smaller salmon-colored spheres representing H.

To carry out a rigorous analysis of the dynamic stability, we have determined the phonon-dispersion relation for a range of different pressure values (Fig. 3) using the ABINIT code. As a test of the accuracy of the latter code, we calculated the pressure-volume relation with ABINIT and compared it with the results obtained from the VASP code. As it can be seen from Fig. 1, ABINIT slightly underestimates the pressure for a given volume when compared to results obtained from VASP but overall the two approaches yield indeed very similar results, strengthening the confidence in the reliability of the data obtained with ABINIT in the following.

Figure 3 shows the dynamical stability of the cubic phase in the high-pressure regime. The stabilized phonon modes in Fig. 3(a) are divided into two parts: the lower band, ranging up to 13 THz, is mostly attributed due to Al while the higher band is formed by H-H and Al-H interactions. For lower pressure values [Fig. 3(b)], it can be clearly seen that the lowest *X* mode becomes soft and eventually turns imaginary, which can be regarded as the precursor of a phase transition. The plot of the *X* mode as a function of pressure shown in Fig. 3(c) illustrates that the cubic phase of AlH_3 can only exist in the pressure range from about 72–106 GPa. Our prediction for the lower pressure limit is in excellent agreement with the result (73 GPa) from a previous theoretical work.[1] The above mentioned slight underestimate of pressure

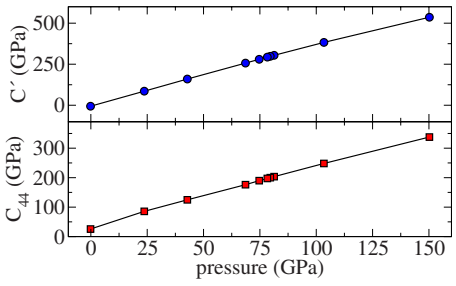

FIG. 2. (Color online) The tetragonal and trigonal shear elastic constants $C'=(C_{11}-C_{12})/2$ and C_{44} are plotted as a function of pressure.

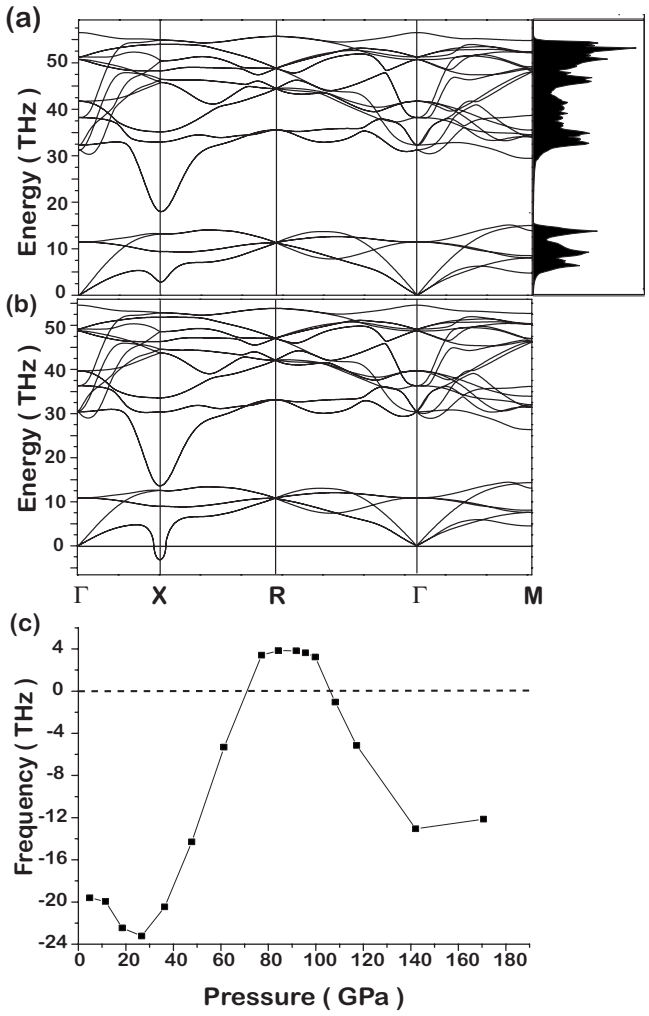

FIG. 3. The phonon-dispersion relation is shown for pressure of (a) 93 GPa and (b) for 70 GPa. The complete evolution of the *X* phonon mode softening is shown in (c) where it becomes apparent that for pressure values below 72 GPa and above 106 GPa the frequency becomes negative (imaginary), indicating the onset of dynamic instability and structural transition to different phases.

calculated with ABINIT as compared to VASP helps to explain why our results indicate a stability island for cubic AlH_3 at a somewhat lower pressure than that reported[2] from VASP results.

As it was recently suggested by Goncharenko *et al.*,[2] the Fermi-surface nesting is dominant at 110 GPa with a significant nesting vector in the *R*–*M* direction, whose transferred momentum is $X\equiv(\frac{1}{2}00)$ at this pressure. The mechanism driving the softening of the *X* mode phonon is closely related with the electronic momentum transfer from *M* $(0\frac{1}{2}\frac{1}{2})$ to *R* $(\frac{1}{2}\frac{1}{2}\frac{1}{2})$ (and vice versa). At the edges of the stability island in Fig. 3(c), the transverse-acoustic (TA) mode at the *X* point, transferring momentum between *M* and *R*, becomes softened. The minimum of the conduction band lies at the *R* point and the highest point of the valence bands lies at *M*. This momentum transfer corresponds to an electron-phonon coupling, which is responsible for the structural instability in this phase.

We find that for ambient pressure and zero temperature

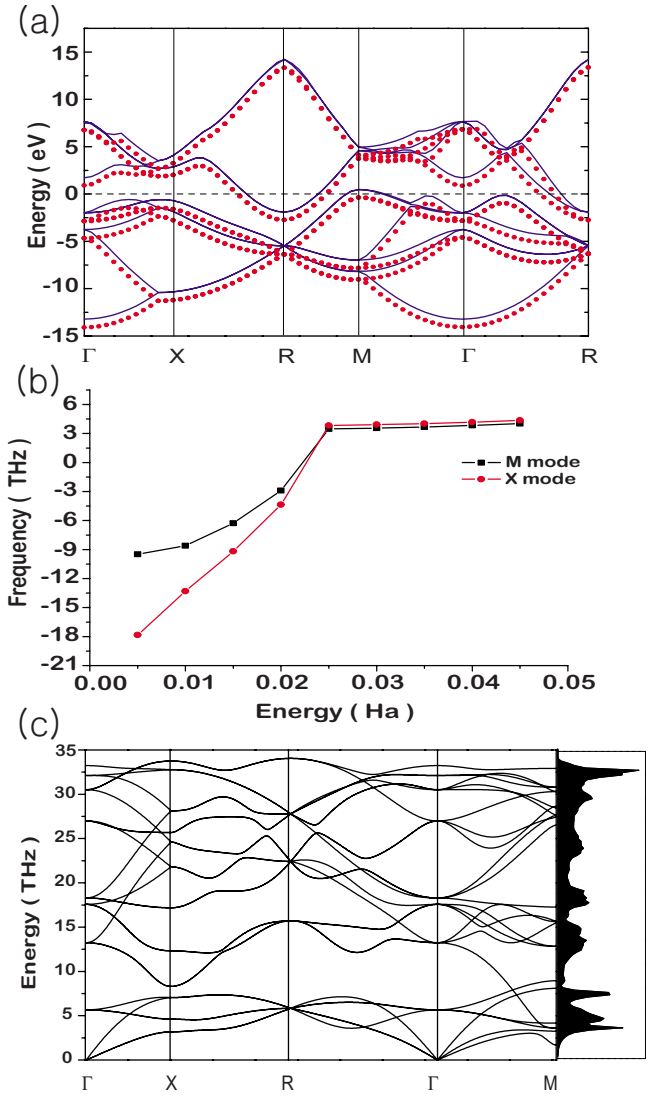

FIG. 4. (Color online) (a) Electronic band structure for zero temperature (solid line) and for 0.040 Ha (red dots). (b) The frequency of the phonon mode at special k points X and M is plotted as a function of the electronic temperature T_e. For $T_e > 0.025$ Ha the frequency is found to become positive (real). (c) Phonon dispersion relation and density of states for $T_e = 0.025$ Ha and 4 GPa pressure.

the phonon dispersion of the cubic phase exhibits imaginary frequencies. As it has been demonstrated previously,[27] such instabilities can often be removed when a finite electronic temperature T_e is taken into account.

We find that the imaginary frequencies at special k points X and M disappear when the electronic temperature T_e is raised to 0.025 Ha [Fig. 4(b)]. At this electronic temperature value, the entire phonon-dispersion relation was calculated by us and it was found that instabilities cease to exist [Fig. 4(c)]. Thus, we can conclude that a finite temperature could indeed lead to the desired stabilization effect in the cubic phase of AlH_3 at ambient pressure.

One can see from the electronic band structure that at the k point M there is a crossing of the Fermi energy level, and at (0.1607, 0.1607, 0) and at (0.1607, 0.1607, 0.1607), we observe a near crossing of the Fermi energy for zero temperature [Fig. 4(a)]. When finite-temperature effects are considered, the Fermi level rises, which results in an effective downward shift for the energy levels away from the Fermi level. This trend will eventually remove the crossing of the Fermi energy level and lead to a stabilization of the cubic phase. Figure 4(b) highlights the stabilized behavior at the special symmetry points M and X with respect to electronic temperature introduced through FD statistics. It is worth noting that the pressure rises up to 8 GPa from the ambient pressure, as would be expected when the electronic temperature is increased at constant volume.

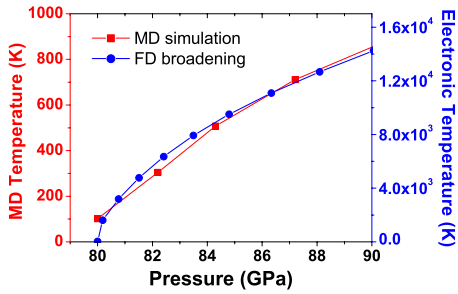

FIG. 5. (Color online) The effect of rising temperature on the pressure for the cubic phase of AlH_3. MD simulation results obtained with VASP code are plotted as red colored square symbols, and ionic relaxation results with Fermi-Dirac broadening scheme as implemented in ABINIT code are plotted as blue solid circles.

Once the phase has been stabilized, the frequencies at special k points M and X remain virtually constant with increasing electronic temperature [Fig. 4(b)], implying that the ion-ion interaction stays mostly unaffected by the elevation of the electronic temperature T_e. This behavior is expected since an increase in T_e entails an almost rigid downshift in the electronic band structure without any new crossings of the Fermi energy occurring and the phase instability that arises from Fermi-surface nesting thus no longer prevails.

One way to arrive at a more physical interpretation of the electronic temperature is to calculate the effect on the pressure at a fixed volume from both molecular-dynamics (MD) simulation and from the FD broadening. To this end, we plot in Fig. 5 the respective temperatures of MD and FD versus calculated pressure. As can be seen, the two plots become aligned to a very good degree when the electronic temperature (FD broadening) is scaled[28] by a factor of approximately 1/17. Taking this result and the above determined minimum electronic temperature of 0.025 Ha (approximately 7900 K) into consideration, one could expect an onset of dynamical stabilization of the cubic phase at ambient pressure for temperatures above approximately 470 K.

In summary, we have shown from density functional theory calculations that the cubic phase of AlH_3 is both mechanically and dynamically stable in the pressure range of 72–106 GPa, in excellent agreement with the recent report by Pickard and Needs[1] who found a transition pressure of 73 GPa based on enthalpy calculations. Combined with their results, we can conclude that the cubic phase of AlH_3 is both energetically and dynamically stable above the transition

pressure. Our results are also consistent with a recent combined experiment-theory work[2] in that a wave vector connecting the points R and M on the Fermi surface undergoes an abrupt change of the electronic screening of the atomic vibration (in the present case, along the X mode). In our calculations, this phonon mode softening is found to occur exclusively in the pressure range from 72 to 106 GPa. At ambient pressure, the cubic structure cannot exist as a ground-state phase. However, once a finite electronic temperature is considered, we find that the phase can indeed become stabilized. Thus, it may be possible that the metallic cubic phase of AlH_3 could be prepared via high-pressure quenching (as we have already demonstrated successfully in the past for another system[12]), and could thus exist even at ambient pressure. Experiments aiming to achieve such a stabilization via a quenching scheme are currently underway.[29]

We would like to acknowledge STINT, VR, FUTURA, Göran Gustafsson Stiftelse, and Wenner-Gren Stiftelserna for financial support, as well as SNIC and UPPMAX for providing computing time. We also thank the anonymous referees and Chris J. Pickard (Univ. of St Andrews) for sharing his structural data with us.

*Duck.Young.Kim@fysik.uu.se
†Rajeev.Ahuja@fysik.uu.se

[1] C. J. Pickard and R. J. Needs, Phys. Rev. B **76**, 144114 (2007).
[2] I. Goncharenko, M. I. Eremets, M. Hanfland, J. S. Tse, M. Amboage, Y. Yao, and I. A. Trojan, Phys. Rev. Lett. **100**, 045504 (2008).
[3] X. Li, A. Grubisic, S. T. Stokes, J. Cordes, G. F. Ganteför, K. H. Bowen, B. Kiran, M. Willis, P. Jena, R. Burgert, and H. Schnöckel, Science **315**, 356 (2007).
[4] P. J. Roach, A. C. Reber, W. H. Woodward, S. N. Khanna, and A. W. Castleman, Jr., Proc. Natl. Acad. Sci. U.S.A. **104**, 14565 (2007).
[5] V. A. Yartys, R. V. Denys, J. P. Maehlen, C. Frommen, M. Fichtner, B. M. Bulychev, and H. Emerich, Inorg. Chem. **46**, 1051 (2007).
[6] J. Graetz, S. Chaudhuri, Y. Lee, T. Vogt, J. T. Muckerman, and J. J. Reilly, Phys. Rev. B **74**, 214114 (2006).
[7] D. Chandra, J. J. Reilly, and R. Chellappa, JOM **58**, 26 (2006).
[8] X. Ke, A. Kuwabara, and I. Tanaka, Phys. Rev. B **71**, 184107 (2005).
[9] C. Wolverton, V. Ozoliņš, and M. Asta, Phys. Rev. B **69**, 144109 (2004).
[10] R. H. Scheicher, D. Y. Kim, S. Lebègue, B. Arnaud, M. Alouani, and R. Ahuja, Appl. Phys. Lett. **92**, 201903 (2008).
[11] D. Y. Kim, J. S. de Almeida, L. Koči, and R. Ahuja, Appl. Phys. Lett. **90**, 171903 (2007).
[12] L. S. Dubrovinsky, N. A. Dubrovinskaia, V. Swamy, J. Muscat, N. M. Harrison, R. Ahuja, B. Holm, and B. Johansson, Nature (London) **410**, 653 (2001).
[13] J. P. Perdew, J. A. Chevary, S. H. Vosko, K. A. Jackson, M. R. Pederson, D. J. Singh, and C. Fiolhais, Phys. Rev. B **46**, 6671 (1992).
[14] P. Hohenberg and W. Kohn, Phys. Rev. **136**, B864 (1964).
[15] W. Kohn and L. J. Sham, Phys. Rev. **140**, A1133 (1965).
[16] P. E. Blöchl, Phys. Rev. B **50**, 17953 (1994).
[17] G. Kresse and J. Furthmüller, Comput. Mater. Sci. **6**, 15 (1996).
[18] G. Kresse and D. Joubert, Phys. Rev. B **59**, 1758 (1999).
[19] H. J. Monkhorst and J. D. Pack, Phys. Rev. B **13**, 5188 (1976).
[20] X. Gonze, Phys. Rev. B **55**, 10337 (1997).
[21] S. Baroni, S. de Gironcoli, and A. Dal Corso, Rev. Mod. Phys. **73**, 515 (2001).
[22] X. Gonze, J.-M. Beuken, R. Caracas, F. Detraux, M. Fuchs, G.-M. Rignanese, L. Sindic, M. Verstraete, G. Zerah, F. Jollet, M. Torrent, A. Roy, M. Mikami, Ph. Ghosez, J.-Y. Raty, and D. C. Allan, Comput. Mater. Sci. **25**, 478 (2002).
[23] D. M. Ceperley and B. J. Alder, Phys. Rev. Lett. **45**, 566 (1980).
[24] N. Troullier and J. L. Martins, Solid State Commun. **74**, 613 (1990).
[25] F. Birch, Phys. Rev. **71**, 809 (1947).
[26] F. Birch, J. Geophys. Res. **83**, 1257 (1978).
[27] V. Recoules, J. Clérouin, G. Zérah, P. M. Anglade, and S. Mazevet, Phys. Rev. Lett. **96**, 055503 (2006).
[28] The underlying reason why the electronic temperature should be downscaled is of course that, unlike molecular-dynamics simulations, the relaxation scheme of density functional theory does not include the kinetic term of ionic motion. Due to this lack of the kinetic term, the force exerted on the ions is mainly originating from the Fermi-Dirac electronic temperature effect on the ionic motion via the Hellmann-Feynman force theorem, which comes from the integration of electronic density and the first derivative of electron-nucleus interaction.
[29] L. Dubrovinsky (private communication).